Available online at www.sciencedirect.com
SCIENCE DIRECT®
ELSEVIER
International Journal of Solids and Structures 43 (2006) 2037–2049
INTERNATIONAL JOURNAL OF SOLIDS and STRUCTURES
www.elsevier.com/locate/ijsolstr

Slip zone length at the edge of a complete contact

C.M. Churchman, D.A. Hills *

Department of Engineering Science, University of Oxford, Parks Road, OX1 3PJ Oxford, United Kingdom

Received 9 December 2004; received in revised form 28 June 2005
Available online 8 September 2005

Abstract

In this paper we solve for the length of the slip zone emanating from the edge of a 90° semi-infinite contact which is nominally adhered to an elastically similar half-plane but has a small region of slip close to the edge. The solution is found using the monolithic three-quarter plane as the basic solution, which incorporates the adhered asymptotes as an 'outer' solution, and using a distribution of dislocations to quantify the region of slip, and also to define an inner slipping asymptote. The solution is applied to a finite square block pressed onto an elastically similar half-plane, and compared with a numerically obtained solution.

Keywords: Complete contact; Partial slip; Fretting; Slip; Asymptotes

1. Introduction

Complete contacts do not often arise in engineering practice, but one example is the spline connection between split shafts in a gas turbine, where the two mating parts are conforming involutes with abrupt edges. The problem of devising a procedure for design against fretting fatigue in these assemblies has prompted an investigation of the qualities of the near-edge tractions-state and attendant state of stress in complete contacts. Because complete contacts invariably have singular states of stress adjacent to the contact edges, asymptotic procedures are valuable in capturing the local pressure and state of stress. We have recently considered slipping contacts by using the Gdoutos and Theocaris (1975) and Comninou (1976) solutions, and it is clear that, when the coefficient of friction is sufficiently high to maintain adhesion, the classical Williams monolithic wedge solution (Williams, 1952) may be employed to represent the contact pair (Mugadu and Hills, 2002). However, although this simple and straightforward application of the

* Corresponding author. Tel.: +44 1865 273119; fax: +44 1865 273813.
E-mail address: david.hills@eng.ox.ac.uk (D.A. Hills).

0020-7683/$ - see front matter
doi:10.1016/j.ijsolstr.2005.06.099

asymptotic solutions is useful, it does not help track out the complete sequence of stress states if the contact is subject to cyclic shear. Mugadu and Hills (2003) examined a problem suffering this loading history for the case when one contacting body is rigid and the other, capable of idealisation as a half-plane, is incompressible. However, this particular problem has the unique property that the order of singularity associated with the two adhered singular eigensolutions and that for the slipping eigensolution are all the same (square root singular), and this gives rise to a straightforward stick-slip regime not exhibited by contact between elastically similar bodies.

In this paper, we describe one step in developing a full description of the contact-edge state of stress when a complete contact is subject to constant normal load and oscillatory shear: we shall examine the case when the coefficient of friction is insufficient to maintain adhesion adjacent to the contact edges, but the slip zones present are small. This affords a description of the slip zone in terms of an outer asymptotic solution which itself represents adhesion.

2. Properties of asymptotes

If the contact edge is adhered the local state of stress may be described by Williams' asymptotic method, a full description of which is given by Barber (1992). If the internal angle of the contact adjacent to the edge is φ, and $\varphi < \pi$, there are two independent singular eigensolutions provided that $\varphi > 77.4°$. These uncouple along the 'notch' bisector, see Fig. 1(a), and it is usual to scale the base solutions so that, along this line, the circumferential stress associated with the more singular eigensolution is unity, and the shear stress associated with the weaker but still singular eigensolution is also unity. It is preferable when these solutions are

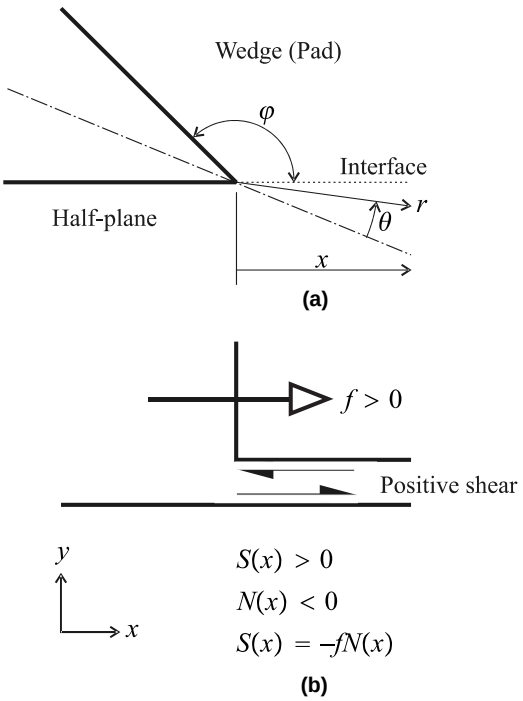

Fig. 1. (a) General wedge geometry of angle φ, (b) sign convention for the coefficient of friction, f: positive for slip of the wedge away from its apex (inwards right relative to the half-plane).

employed in contact problems to re-scale the base solutions so that the contact pressure arising along the interface, represented by each term, is unity, i.e.,

$$p(r) = K_{\mathrm{I}}^0 r^{\lambda_{\mathrm{I}}-1} + K_{\mathrm{II}}^0 r^{\lambda_{\mathrm{II}}-1} \quad \text{on } \theta = \frac{(\pi-\varphi)}{2}, \tag{1}$$

where λ_{I}, λ_{II} are given by the solutions to the following two equations:

$$\lambda_{\mathrm{I}} \sin(\pi+\varphi) + \sin((\pi+\varphi)\lambda_{\mathrm{I}}) = 0, \qquad \lambda_{\mathrm{II}} \sin(\pi+\varphi) - \sin((\pi+\varphi)\lambda_{\mathrm{II}}) = 0, \tag{2}$$

which for the case of a 90° punch on a half plane, $\varphi = \pi/2$, and so $\lambda_{\mathrm{I}} = 0.5445$ and $\lambda_{\mathrm{II}} = 0.9085$. The generalised stress intensity factors, K_{I}^0, K_{II}^0, are found by collocating the solution to whatever finite problem is being studied, whilst the corresponding shear stress is given by

$$q(r) = K_{\mathrm{I}}^0 r^{\lambda_{\mathrm{I}}-1} g_{r\theta}^{\mathrm{I}} + K_{\mathrm{II}}^0 r^{\lambda_{\mathrm{II}}-1} g_{r\theta}^{\mathrm{II}}, \tag{3}$$

where the functions $g_{r\theta}^{\mathrm{I}}$, $g_{r\theta}^{\mathrm{II}}$ are provided by the eigenvectors to Williams' problem. For the example case of $\varphi = \pi/2$, we have $g_{r\theta}^{\mathrm{I}} = 0.543$ and $g_{r\theta}^{\mathrm{II}} = -0.219$. It is not possible to provide all the algebra here, for which the original papers should be consulted.

If the contact edge is slipping the Gdoutos and Theocaris (1975) and Comninou (1976) solution applies. The coefficient of friction is denoted f, chosen to be a positive quantity if the contact is slipping inwards relative to the half-plane, and a negative quantity if the contact is slipping outwards. This ensures that positive shearing tractions arise (corresponding to inward slip) when the coefficient of friction is positive and the normal stress is compressive/negative, and $S(x) = -fN(x)$, see Fig. 1(b). The local traction distribution is still power order in form

$$p(x) = \frac{q(x)}{-f} = K_{\mathrm{s}} x^{\lambda_{\mathrm{s}}-1}, \tag{4}$$

but with a solitary singular term, and the eigenvalue λ_{s} is shown in Fig. 2. The plot includes the values of the two singular eigensolutions for the adhered problem, λ_{I}, λ_{II}, for comparison. In the region of relevance here, $-f < 0.543$, we note that $\lambda_{\mathrm{I}} < \lambda_{\mathrm{s}} < \lambda_{\mathrm{II}}$.

Now, it will be noted that, if the contact is truly complete and also adhered, as the contact edge is approached ($r \to 0$) the solution is dominated by the more singular term, and hence, to preserve a compressive contact pressure we require that $K_{\mathrm{I}}^0 < 0$. The direction in which slip is allowed is also restricted by the form

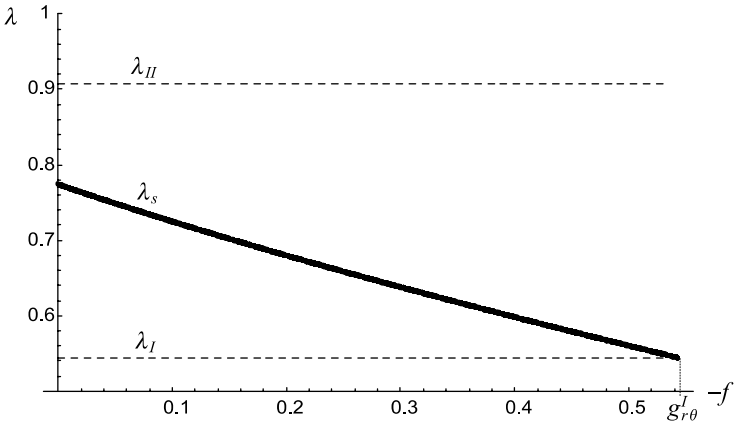

Fig. 2. Plot showing λ_{s} as a function of the coefficient of friction, f, for slip away from the apex (i.e., in the negative f direction). Also included are the λ_{I},λ_{II} values for the adhered case.

of the adhered asymptotes. As we define $q(x)/p(x) = -f$ and we know that within the asymptote, $q(x)/p(x) = g^{\mathrm{I}}_{r\theta}$ (as we approach the apex, $x \to 0$), where $g^{\mathrm{I}}_{r\theta} = +0.543$ we must have $f < 0$, implying that slip must be outwards (in the negative f direction as defined in Fig. 1(b)), regardless of the combination of applied loads. It also means that the shearing traction distribution at the edge is dominated by the lead singular term, and hence slip will be prevented if $|f| > g^{\mathrm{I}}_{r\theta}$, i.e., for a punch with a right-angle edge, if $|f| > 0.543$. If the coefficient of friction is lower than this the contact edge will certainly slip, and in this paper we shall be concerned with contacts where the coefficient of friction is less than the critical value for adhesion.

3. Example problem

Complete contacts inevitably require elasticity formulations appropriate to finite bodies, and hence are not amenable to closed form solution. Further, it is formally impossible to separate the contact problem from the load path distribution in the body as a whole, and this means that all contact pressure distributions are geometry-specific. With this in mind we studied the simplest possible complete contact using the finite element method, and this is shown in Fig. 3: it depicts an elastic square of side $2a$ pressed into an elastically similar half-plane by uniform pressure on the upper surface equivalent to a normal contact load P, and where a shearing force, Q, in the plane of the interface, may also be developed. The interface has a coefficient of friction, f. When a normal load alone is applied, if $|f| > g^{\mathrm{I}}_{r\theta}$, the entire punch face sticks. However, if this inequality is not satisfied the central region of the contact sticks whilst slip zones, of opposite sign, attached to the edges, appear. These are of fixed extent. The problem has similarities with the celebrated Spence problem (Spence, 1973) of contact between a flat-ended rigid indenter and an elastic half plane, but here the reason for the development of tangential slip displacement is the different domains representing the contacting bodies, rather than elastic mismatch.

If a monotonically increasing shear force is now imposed, one slip region, viz. that attached to the trailing edge sticks, whilst the other increases in size. Considering, first, the effect of a normal load alone, we note that, for values of the coefficient of friction close to $g^{\mathrm{I}}_{r\theta}$, the slip regions are relatively small in extent. It is also quite hard to find their size explicitly, as both components of traction become power order singular

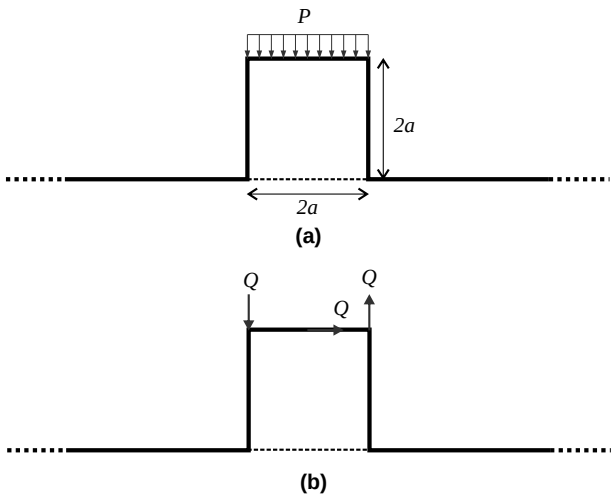

Fig. 3. Geometry of the FEM problem: Square block of side $2a$ pressed onto an elastically similar half-plane with (a) pressure applied and (b) shear force applied.

in these neighbourhoods, and it is difficult to achieve convergence using the finite element method. The question arises whether an alternative approach, of more widespread applicability, is possible, if the slip zones are indeed small in size compared with the region in which the singular terms associated with adhesion dominate the problem. It is therefore proposed that a self-contained solution for slip adjacent to the edge of a contact between a semi-infinite wedge (which may, as here, be of internal angle $\pi/2$ radians, and hence a quarter plane), is pressed into a half-plane. This would imply that the input variables to the problem would be the generalised stress intensity factors, K_{I}^0, K_{II}^0, together with the coefficient of friction, f. Note that, in order for the contact to be maintained right up to the wedge-edge, we require $K_{\mathrm{I}}^0 < 0$, Eq. (1). The actual generalised stress intensity factors for the problem under consideration, *assuming complete adhesion*, were found from the finite element output, and are given by

$$\begin{Bmatrix} K_{\mathrm{I}}^0 a^{\lambda_{\mathrm{I}}-1} \\ K_{\mathrm{II}}^0 a^{\lambda_{\mathrm{II}}-1} \end{Bmatrix} = \begin{bmatrix} -0.157 & 0.179 \\ -0.130 & -0.274 \end{bmatrix} \begin{Bmatrix} P/2a \\ Q/2a \end{Bmatrix}. \tag{5}$$

4. Formulation

The problem to be solved within the context of a semi-infinite asymptote, is shown in Fig. 4. It consists of an elastic quarter plane, pressed onto an elastically similar half plane, and possibly subject to an external

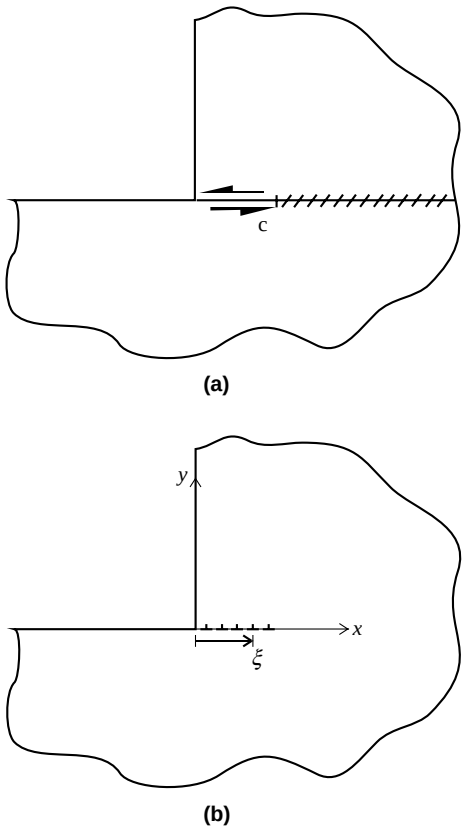

Fig. 4. Geometry of three-quarter plane slip zone, (a) showing slip zone extent, (b) showing dislocation distribution along x-axis.

shear. The majority of the interface, save for a small region adjacent to the contact corner, is adhered. The loading is represented by the first two (singular) terms of a Williams asymptotic expansion for a notch forming a three-quarter plane, but written down so as to give emphasis to the contact interface (Eqs. (1) and (3)). The expressions for $p(x)$, $q(x)$ implied by these equations are true at significant distances from the corner, i.e., $x \gg c$ (which are still small compared with other dimensions of the body), but there is a region, of initially unknown extent (c), where slipping occurs. The solution is found by distributing glide dislocations (see Hills et al., 1996) along the interface within this interval, in order to enforce the friction law, i.e.,

$$\begin{aligned} S(x) &= -fN(x) \quad 0 \leqslant x \leqslant c \\ &< -fN(x) \quad x > c, \end{aligned} \tag{6}$$

where the direct and shear tractions, $N(x)$, $S(x)$ are given by

$$N(x) = K_{\mathrm{I}}^{0} x^{\lambda_{\mathrm{I}}-1} + K_{\mathrm{II}}^{0} x^{\lambda_{\mathrm{II}}-1} + \frac{2\mu}{\pi(\kappa+1)} \int_0^c B_x(\xi) F_{xyy}(x,\xi)\,\mathrm{d}\xi, \tag{7}$$

$$S(x) = K_{\mathrm{I}}^{0} g_{r\theta}^{\mathrm{I}} x^{\lambda_{\mathrm{I}}-1} + K_{\mathrm{II}}^{0} g_{r\theta}^{\mathrm{II}} x^{\lambda_{\mathrm{II}}-1} + \frac{2\mu}{\pi(\kappa+1)} \int_0^c B_x(\xi) \left[F_{xxy}(x,\xi) + \frac{1}{x-\xi} \right] \mathrm{d}\xi, \tag{8}$$

μ is the modulus of rigidity, κ Kolsov's constant, $B_x(\xi) = \mathrm{d}b_x/\mathrm{d}x$ the dislocation density, and $F_{ijk}(x,\xi)$ the influence function connecting stress component $\sigma_{jk}(x)$ due to a dislocation $b_i(\xi)$, present on the projection line of a three-quarter plane. Details of the derivation of these functions are given in Churchman et al. (in press), and a summary of the functions given in the appendix. Substituting the two integral representations into the friction law, Eq. (6), leads to the following Cauchy singular integral equation for the unknown dislocation density:

$$(f + g_{r\theta}^{\mathrm{I}}) \left(\frac{x}{d_0} \right)^{\lambda_{\mathrm{I}}-1} + (f + g_{r\theta}^{\mathrm{II}}) \left(\frac{x}{d_0} \right)^{\lambda_{\mathrm{II}}-1} + \int_0^c \widehat{B}_x(\xi) F_T(f,x,\xi)\,\mathrm{d}\xi = 0 \quad \text{for } 0 \leqslant x \leqslant c, \tag{9}$$

where

$$F_T(f,x,\xi) = fF_{xyy}(x,\xi) + F_{xxy}(x,\xi) + \frac{1}{x-\xi}, \tag{10}$$

$$\widehat{B}_x(\xi) = \frac{2\mu}{\pi(\kappa+1)} \frac{B_x(\xi)}{K_{\mathrm{I}}^{0} d_0^{\lambda_{\mathrm{I}}-1}}, \tag{11}$$

and

$$d_0 = \left(\frac{K_{\mathrm{I}}^{0}}{K_{\mathrm{II}}^{0}} \right)^{\frac{1}{\lambda_{\mathrm{II}}-\lambda_{\mathrm{I}}}}. \tag{12}$$

The last quantity, d_0, is particularly noteworthy as it indicates that the problem has an inherent length scale, introduced by dint of the two generalised stress intensity factors having different units, i.e., the units of K_{I}^{0} are $[FL^{-(1+\lambda_{\mathrm{I}})}]$ and those of K_{II}^{0} are $[FL^{-(1+\lambda_{\mathrm{II}})}]$. Therefore, as d_0 represents the only length dimension in a semi-infinite wedge solution, it is appropriate to normalise coordinates with respect to this value. Note that its magnitude depends directly on the two stress intensity factors, and therefore on the loading mix, but also (via λ_{I} and λ_{II}) on the geometry. Here, because we are restricting attention to the case of a punch having edge angle $\pi/2$, $\lambda_{\mathrm{II}} - \lambda_{\mathrm{I}} = 0.364$, but if a punch with larger interior edge angle were being considered this difference would be rather smaller. Let

$$\hat{x} = \frac{x}{d_0}, \qquad \hat{c} = \frac{c}{d_0}, \qquad \hat{\xi} = \frac{\xi}{d_0}, \tag{13}$$

so that the integral equation becomes

$$(f+g^{\mathrm{I}}_{r\theta})\hat{x}^{\lambda_{\mathrm{I}}-1}+(f+g^{\mathrm{II}}_{r\theta})\hat{x}^{\lambda_{\mathrm{II}}-1}+\int_0^{\hat{c}}\widehat{B}_x(\hat{\xi})F_T(f,\hat{x},\hat{\xi})\,\mathrm{d}\hat{\xi}=0\quad\text{for } 0\leqslant\hat{x}\leqslant\hat{c}, \tag{14}$$

and carry out a further stage in normalisation, to place the integral over the standardised range $[-1,1]$, by letting

$$\hat{\xi}=\frac{\hat{c}}{2}(u+1), \tag{15}$$

$$\hat{x}=\frac{\hat{c}}{2}(v+1). \tag{16}$$

This gives

$$\int_{-1}^{+1}\widehat{B}_x(u)G_T(f,v,u)\,\mathrm{d}u = -(f+g^{\mathrm{I}}_{r\theta})\left(\frac{\hat{c}}{2}\right)^{\lambda_{\mathrm{I}}-1}(v+1)^{\lambda_{\mathrm{I}}-1}-(f+g^{\mathrm{II}}_{r\theta})\left(\frac{\hat{c}}{2}\right)^{\lambda_{\mathrm{II}}-1}(v+1)^{\lambda_{\mathrm{II}}-1}\quad\text{for } -1\leqslant v\leqslant+1. \tag{17}$$

5. Solution

The first step in the inversion procedure is to prescribe the fundamental form of the solution. We expect a smooth transition from slip to stick, and therefore bounded behaviour of the dislocation density as $u\to+1$, whilst at the corner, as $u\to-1$, the state of stress varies as x^{λ_s-1}, i.e., it is singular in character (but not square root singular: λ_s is given in Fig. 2). Standard procedures for inversion of Cauchy integral equations, derived from the Riemann–Hilbert procedure, require the exponents of the end point behaviour to add up to -1, 0, 1. Here, the equation has a generalised Cauchy kernel, and so, strictly speaking, the Riemann–Hilbert procedure does not apply, and hence the exponents do not have this property. Nevertheless, experience has shown that convergence can usually be readily achieved, even when the order of singularity is not precisely matched. We shall therefore choose a fundamental function which *does* assume square root singular behaviour when $u\to-1$. The discrepancy between the actual order of the singularity and this assumed form is smallest when $-f\to g^{\mathrm{I}}_{r\theta}$, and hence the solution developed converges rapidly if $-f>0.4$, so that $\lambda_s-1\lesssim-0.4$. An alternative fundamental function, $w(u)$, and hence quadrature, would be needed for lower values of $|f|$ (where λ_s-1 is very different from -0.5) but here the slip zone is so large that the hinterland is no longer dominated by the K^0_{I}, K^0_{II} field, and so the issue does not arise. We therefore let

$$\widehat{B}_x(u)=\phi(u)w(u),$$

where

$$w(u)=\sqrt{\frac{1-u}{1+u}}. \tag{18}$$

A numerical inversion is needed, and the appropriate quadratures are described in Erdogan et al. (1973) or Conte and De Boor (1972). The integration points, u_i and the collocation points v_k are given by

$$u_i=\cos\left(\pi\frac{2i}{2n+1}\right)\quad\text{for } i=1,\ldots,n, \tag{19}$$

$$v_k=\cos\left(\pi\frac{2k-1}{2n+1}\right)\quad\text{for } k=1,\ldots,n, \tag{20}$$

and the integral equation itself becomes

$$\sum_{i=1}^{n} \frac{2\pi(1-u_i)}{2n+1} G_T(f, v_k, u_i)\phi_x(u_i) = -(f+g_{r\theta}^{\mathrm{I}})\left(\frac{\hat{c}}{2}\right)^{\lambda_{\mathrm{I}}-1}(v_k+1)^{\lambda_{\mathrm{I}}-1} - (f+g_{r\theta}^{\mathrm{II}})\left(\frac{\hat{c}}{2}\right)^{\lambda_{\mathrm{II}}-1}(v_k+1)^{\lambda_{\mathrm{II}}-1} \quad \text{for } k=0,\ldots,n. \tag{21}$$

This represents n equations for the n unknowns $\phi_x(u_i)$, but additionally we need to determine the extent of the slip region, $\hat{c}$. Because we have no side condition we must rely on checking the results to ensure that the following inequalities are satisfied:

$$\begin{aligned} &S(x) < |-fN(x)| \quad \text{for } x > c, \\ &\operatorname{sgn}(h(x)) = \operatorname{sgn}(S(x)) \quad \text{for } x \leqslant c, \end{aligned} \tag{22}$$

where $h(x)$ is the tangential displacement or slip displacement:

$$h(x) = \int_{x/c}^{1} B_x(\xi)\,\mathrm{d}\xi. \tag{23}$$

A further known condition, which, in practice, has considerably assisted in establishing the slip interval, is that the traction distribution adjacent to the contact edge ($\hat{x} \ll \hat{c}$) must display a form given by the slipping Comninou asymptote (Eq. (4)), and hence $N(x)$ must vary like x^{λ_s-1} if $x \ll c$. This also provides calibration for the slipping asymptote at the contact edge, i.e.,

$$K_{\mathrm{s}} = \frac{N(x)}{x^{\lambda_{\mathrm{s}}-1}} \quad \text{as } x/c \to 0, \tag{24}$$

or, in order to provide a more rational normalisation for the slipping stress intensity,

$$\frac{K_{\mathrm{s}}}{K_{\mathrm{I}}^0 d_0^{\lambda_{\mathrm{I}}-\lambda_{\mathrm{s}}}} = \frac{N(x)}{K_{\mathrm{I}}^0 d_0^{\lambda_{\mathrm{I}}-1}} \frac{1}{\hat{x}^{\lambda_{\mathrm{s}}-1}} \quad \text{as } \hat{x} \to 0. \tag{25}$$

6. Results

The primary output is the size of the slip zone, $\hat{c}$ for a given f. Before presenting the results from solving the integral equation we note that an approximate solution for the stick-slip boundary may be found from the adhered asymptotic solution alone, by determining the distance over which the friction law is exceeded, and which will be denoted by c_0. Setting $S(c_0) = -fN(c_0)$ we find that

$$(f+g_{r\theta}^{\mathrm{I}})\left(\frac{c_0}{d_0}\right)^{\lambda_{\mathrm{I}}-1} + (f+g_{r\theta}^{\mathrm{II}})\left(\frac{c_0}{d_0}\right)^{\lambda_{\mathrm{II}}-1} = 0, \tag{26}$$

$$\frac{c_0}{d_0} = \left\{-\frac{(f+g_{r\theta}^{\mathrm{I}})}{(f+g_{r\theta}^{\mathrm{II}})}\right\}^{\frac{1}{\lambda_{\mathrm{II}}-\lambda_{\mathrm{I}}}}. \tag{27}$$

In Fig. 5 the first estimate of the slip zone (c_0/d_0) is shown, together with the numerical solution $\hat{c}$ (= c/d_0) as a function of the coefficient of friction. It will be seen that the true slip distance, $\hat{c}$, is a constant multiple of approximate solution. Specifically:

$$\frac{c}{d_0} = 2.4\frac{c_0}{d_0}.$$

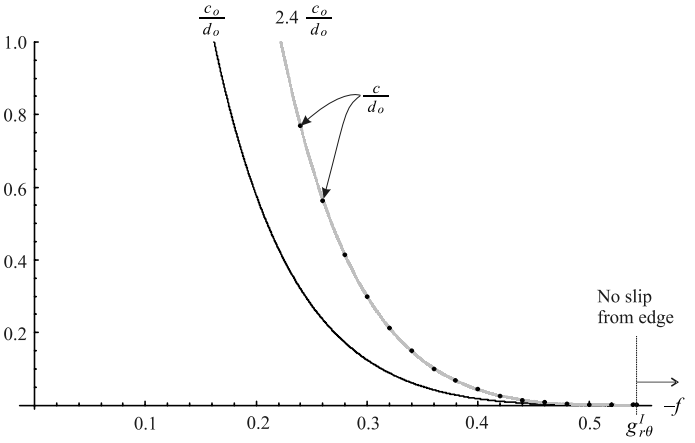

Fig. 5. Plot showing both $\frac{c_0}{d_0}$ and $\frac{c}{d_0}$, as a function of the coefficient of friction, f, for slip away from the apex (i.e., in the negative f direction).

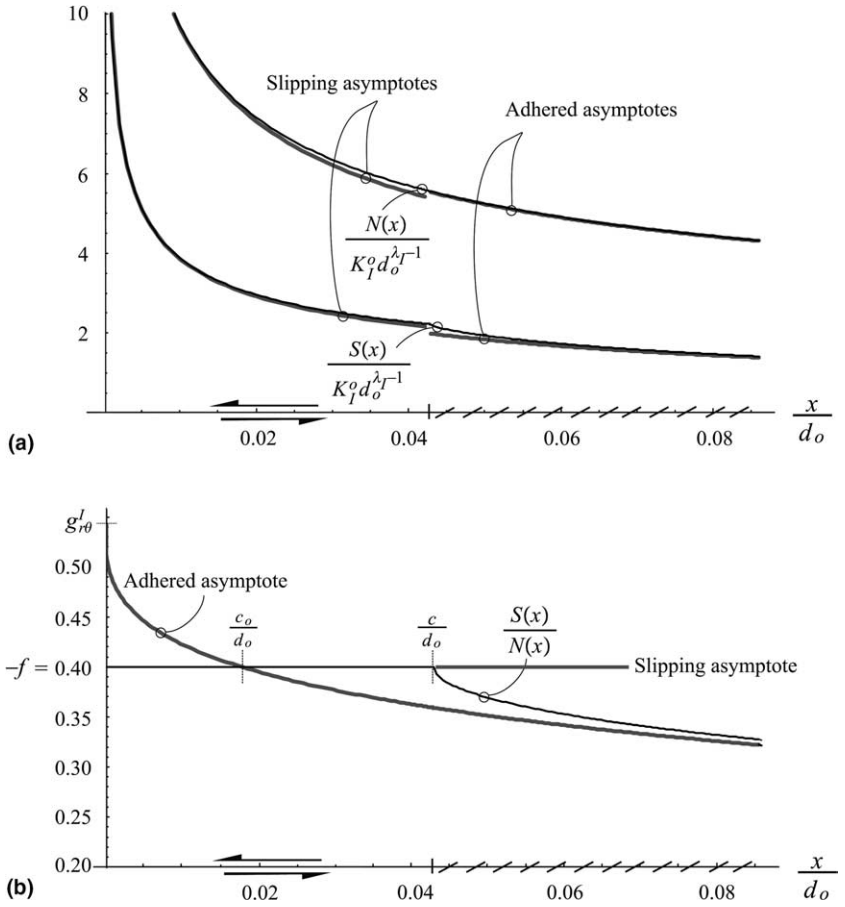

Fig. 6. Plots of the tractions $N(x)$, $S(x)$ for the asymptote derived, together with the adhered inner solution and slipping asymptote adjacent to the edge. The two figures are equivalent, but (a) is the raw tractions and (b) their ratio which emphasises the difference between them. $f = -0.4$.

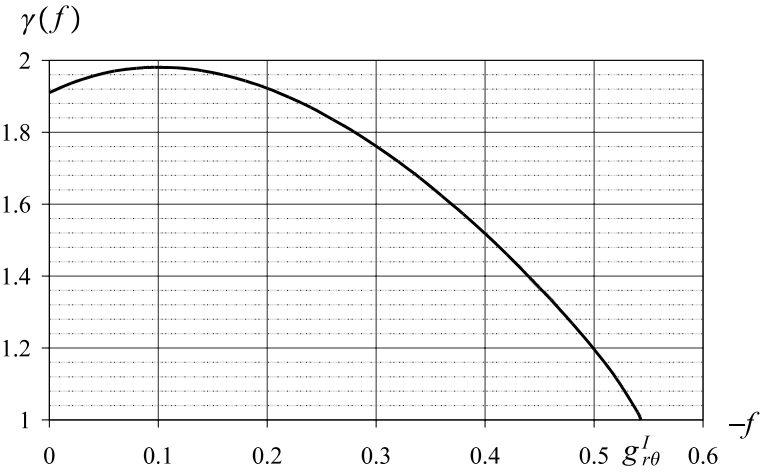

Fig. 7. Plot of $\gamma(f)$ against f where $\gamma(f) = \frac{K_s}{K_I^0 d_0^{\lambda_I - \lambda_s(f)}}$.

This means that we may produce a crisp formula for the true size of the slip zone for a 90° wedge pressed onto a half plane:

$$c = 2.4\left\{ -\frac{(f + g^{\mathrm{I}}_{r\theta})}{(f + g^{\mathrm{II}}_{r\theta})} \frac{K^0_{\mathrm{I}}}{K^0_{\mathrm{II}}} \right\}^{\frac{1}{\lambda_{\mathrm{II}} - \lambda_{\mathrm{I}}}}. \tag{28}$$

Fig. 6 displays the traction distributions within the neighbourhood of the asymptote, normalised as $\frac{N(x)}{K_I^0 d_0^{\lambda_I - 1}}$ and $\frac{S(x)}{K_I^0 d_0^{\lambda_I - 1}}$. We also plot on the figure the adhered 'asymptote to the asymptote', i.e., the traction distributions implied by the Williams solution for $x/c \gg 1$. It should be noted that, as the edge of the contact is approached, i.e., $x/c \ll 1$, the behaviour moves towards the Comninou sliding asymptote. The gradient here has already been used in the numerical part of the solution, and we may collocate the value of the generalised stress intensity factor, K_s, from the numerical results. It is found that

$$K_s = \gamma(f) K^0_{\mathrm{I}} d_0^{\lambda_{\mathrm{I}} - \lambda_s(f)}, \tag{29}$$

$$= \gamma(f) K^0_{\mathrm{I}} \left(\frac{K^0_{\mathrm{I}}}{K^0_{\mathrm{II}}} \right)^{-\frac{\lambda_s(f) - \lambda_{\mathrm{I}}}{\lambda_{\mathrm{II}} - \lambda_{\mathrm{I}}}}, \tag{30}$$

where $\gamma(f)$ is given in Fig. 7 and $\lambda_s(f)$ is given in Fig. 2. As a useful check, we see that if we set $f = -g^{\mathrm{I}}_{r\theta}$ then $\lambda_s(f) = \lambda_{\mathrm{I}}$ and $\gamma(f) = 1$ giving the expected result that $K_s = K^0_{\mathrm{I}}$, i.e., there are no slip zones and the contact remains adhered everywhere. Therefore, there is a smooth transition between slip at the edge and adhesion at the edge. We may also look at the maximum of the $\gamma(f)$ curve and we see that it peaks at $f = -0.09654$ and that at this point $\frac{\lambda_s(f) - \lambda_{\mathrm{I}}}{\lambda_{\mathrm{II}} - \lambda_{\mathrm{I}}} = \frac{1}{2}$ and therefore we have: $K_s = 1.98\sqrt{K^0_{\mathrm{I}} K^0_{\mathrm{II}}}$.

7. Application to example problem

The results found may be applied, as an example, to the square pad pressed onto a half-plane, treated by the finite element method, and described in an earlier section. In order to apply the recipe of the previous section, we note that the input parameters are f, K^0_{I} and K^0_{II}. The latter two may be calibrated, for a given

geometry, with $\frac{Q}{P}$, provided that there are no other slipping regions, the calibrations for K_{I}^0 and K_{II}^0 found earlier may be used. Thus (28) and (29) become, for this particular geometry,

$$\frac{c}{a} = 2.4\left\{-\frac{(f+0.543)}{(f-0.219)}\left(\frac{-0.157+0.179(Q/P)}{-0.130-0.274(Q/P)}\right)\right\}^{\frac{1}{\lambda_{\mathrm{II}}-\lambda_{\mathrm{I}}}}, \tag{31}$$

and

$$K_{\mathrm{s}}a^{\lambda_{\mathrm{s}}(f)-1} = \gamma(f)(-0.157(P/2a)+0.179(Q/2a))\left(\frac{-0.157+0.179(Q/P)}{-0.130-0.274(Q/P)}\right)^{-\frac{\lambda_{\mathrm{s}}(f)-\lambda_{\mathrm{I}}}{\lambda_{\mathrm{II}}-\lambda_{\mathrm{I}}}}. \tag{32}$$

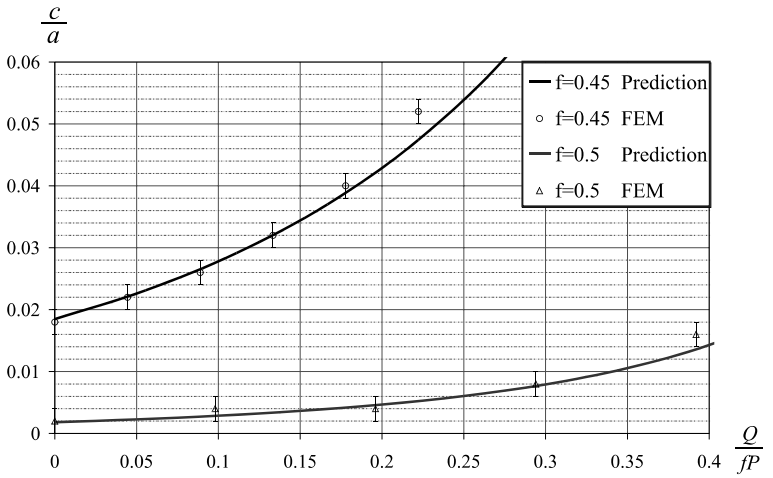

Fig. 8. $\frac{c}{a}$ as a function of $\frac{Q}{fP}$ for $|f| = 0.45$ and $|f| = 0.5$ showing the correlation between the prediction derived from the asymptotes and the FEM output. The latter includes error bars as the output has an oscillatory component.

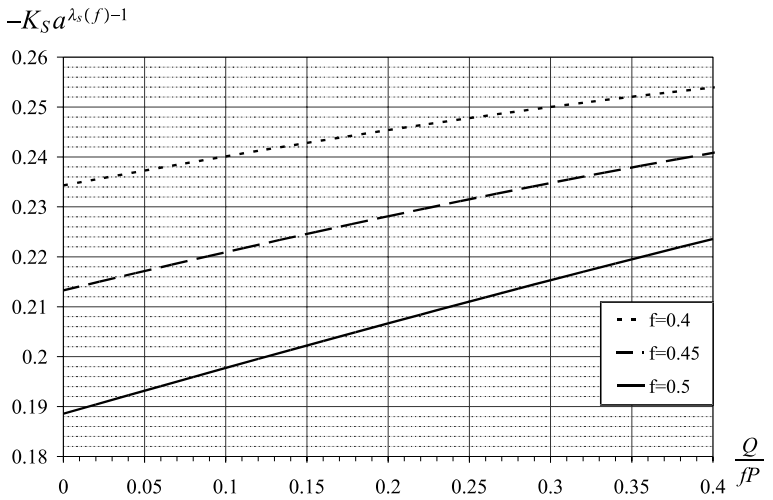

Fig. 9. Plot showing the slipping stress intensity factor, K_{s}, as a function of the loading on the finite problem, $\frac{Q}{fP}$, for coefficients of friction, $|f| = 0.4$, 0.45 and 0.5.

Fig. 8 displays the size of the slip zones c/a predicted by the finite element method,[1] as a function of the shearing force, Q/fP, for constant coefficients of friction (when $Q > 0$ the results apply only to the growing slip zone of course). Using the calibration for the 'full stick' generalised stress intensity factors given above the size of the slip region was found. These predictions are included on the figure and, as expected, show an excellent correlation with the finite element (slipping) solution when $c/a \ll 1$, when the effect of the presence of the opposite free surface of the punch is negligible. For completeness, plots of the slipping stress intensity factor given in Eq. (32) have been included for this particular calibration in Fig. 9.

8. Conclusion

In this paper we show how the edges of sharp contacts, where the interfacial coefficient of friction is less than a critical value may be characterised by two stress intensity factors appropriate to *adhered* behaviour. This permits the size and tractions within an embedded slip region to be found accurately (providing that the coefficient of friction is fairly close to the critical value, $g^{\mathrm{I}}_{r\theta}$, i.e., $0.4 < |f| < 0.543$ and for low Q/fP). The scheme may be employed for contacts with a range of edge angles, but is here developed for the case of a right-angle pad edge.

Appendix

Influence functions. The stress, σ_{ij}, at a position x for an edge dislocation b_k at a distance ξ from the origin of a three-quarter plane (with the term corresponding to a dislocation in an infinite plane omitted)

$$F_{kij}\left(\frac{x}{\xi}\right) = \frac{1}{\left(\frac{x}{\xi}\right)^{1-\lambda_1} + \left(\frac{x}{\xi}\right)^{t}} \sum_{m=0}^{3} C_m \left(\frac{\frac{x}{\xi}}{1+\frac{x}{\xi}}\right)^{m}$$

	t	C_0	C_1	C_2	C_3	$\sum_{m=0}^{3} C_m$
F_{xyy}	1.45	−0.8416	3.602	−3.146	0.6288	0.2427
F_{xxy}, F_{yyy}	1	−0.3650	−0.1416	−3.942	3.450	−0.9986
F_{yxy}	1.45	−0.2726	−1.016	2.333	−0.3687	0.6757

References

Barber, J.R., 1992. Elasticity. Kluwer Academic Publishers, Dordrecht.

Churchman, C.M., Korsunsky, A.M., Hills, D.A., in press. The edge dislocation in a three-quarter plane—Part I: Influence functions. Eur. J. Mech. A/Solids.

Comninou, M., 1976. Stress singularity at a sharp edge in contact problems with friction. J. Appl. Math. Phys. (ZAMP) 27, 493–499.

Conte, S.D., De Boor, C., 1972. Elementary Numerical Analysis, second ed. McGraw-Hill, New York.

Erdogan, F., Gupta, G.D., Cook, T.S., 1973. In: Sih, G.C. (Ed.), Numerical Solution of Singular Integral Equations, Methods of Analysis and Solutions of Crack Problems. Noordhoff, Groningen, pp. 368–425 (Chapter 7).

Gdoutos, E.E., Theocaris, P.S., 1975. Stress concentrations at the apex of a plane interacting on an elastic half-plane. J. Appl. Mech. 42, 688–692.

Hills, D.A., Kelly, P.A., Dai, D.N., Korsunsky, A.M., 1996. Solution of Crack Problems—The Distributed Dislocation Technique. Kluwer Academic Publishers, Dordrecht.

[1] NB: In the finite element model there are 700 elements along the contact surface and the element length close to the corners is $0.002a$.

Mugadu, A., Hills, D.A., 2002. Characterising the process zone in complete fretting contacts using plain fatigue sharp V-notch specimens. J. Mech. Phys. Solids 50, 1417–1429.

Mugadu, A., Hills, D.A., 2003. The evolution of the process zone when a complete contact is subject to cyclically varying loads. Int. J. Solids Struct. 40, 4417–4435.

Spence, D.A., 1973. An eigenvalue problem for elastic contact with finite friction. Proc. Cambr. Philos. Soc. 73, 249–268.

Williams, M.L., 1952. Stress singularities resulting from various boundary conditions in angular corners of plates in extension. J. Appl. Mech. 19, 526–528.